

Self-assembled three-dimensional conducting network of single-wall carbon nanotubes

Graciela B. Blanchet,^{a)} Shekhar Subramoney, R. K. Bailey, and G. D. Jaycox
DuPont, Central Research and Development, Wilmington, Delaware 19880

C. Nuckolls

Columbia University, Chemistry Department, New York, New York, 10027

(Received 11 March 2004; accepted 8 June 2004)

We described here the self-assembling of a three-dimensional array of single-wall nanotubes (SWNTs). The distinctive choice of materials allowed for the self-assembly of SWNTs with low resistance conducting polymer links into a conducting network that when embedded into an insulating host shows no disruption of the conduction path. The ability to control network formation independently of the electrical properties of the host drastically changes the design of these conducting organic networks. Thus, enabling the tailoring of their electrical properties while addressing issues of film processability relevant for their application as printable conductors in organic electronic applications. These networks provide opportunities for applications in micro- and nanoelectronics. © 2004 American Institute of Physics. [DOI: 10.1063/1.1776619]

There is considerable interest in the fabrication of organic electronic devices¹⁻⁴ on flexible substrates. Among the available printing processes, thermal transfer is quite unique. This laser-assisted dry-transfer technique allows for the high-resolution printing of devices over large areas while providing a low-cost path toward the early commercialization of plastic electronics.^{5,6} The printable conductor presented here, a self-assembled three-dimensional array of single-wall nanotubes (SWNTs) is also quite unique. The distinctive choice of materials allowed for the self-assembly of SWNTs with low resistance conducting polymer links into a conducting network that when embedded into an insulating host shows no disruption of the conduction path. The ability to control network formation independently of the electrical properties of the host drastically changes the design of organic conducting networks providing opportunities for applications in micro- and nanoelectronics. While the self-assembled networks of SWNT ropes presented here are suitable printable conductors for thin-film transistor (TFT) applications; self-assembled networks of single tubes may provide a viable path for the fabrication of wires for nanoelectronics.

The synthesis of a material satisfying the transport requirements for a polymeric device is not difficult. However, maintaining the material's electrical integrity throughout the laser-driven printing process is far more challenging. Archetypal conducting organics, such as polyanilines (PANIs)⁷⁻¹⁰ cannot withstand the imaging process deprotonating at fairly modest temperatures.¹¹ Consequently, designing a conductor that is printable via thermal transfer for TFT applications would require maintaining high conductivity but a minimal amount of conducting polymer. We show here that self-assembled networks of SWNT and dinonyl naphthalene sulfonic acid-doped polyaniline (DNNSA-PANI) links embedded in an insulating matrix fulfill such requirements. These networks percolate into a conducting regime with a 10^9 -fold increase in conductivity at very low SWNT concentrations

even when embedded in a highly insulating host, such as polystyrene. Compositional analysis shows that DNNSA-PANI is present only at the tube surface suggesting that the integrity of the self-assembled network is not disrupted when embedded in the polystyrene (PS) host. This indicates that DNNSA-PANI provides low resistance links that effectively connect SWNT along the percolating path.¹² However, as the relative affinity of the host to nanotubes increases, the integrity of the conducting network can be partially or totally disrupted when embedded in the host. The disturbance of the conducting network is reflected by a shift in conductivity and percolation threshold revealing the presence of insulating as well as conducting links.

The polyaniline was prepared as described in Ref. 13. Carbon Nanotubes, Inc. manufactured the nanotubes used in the work via a high-pressure carbon monoxide (HIPCO® SWNT) disproportionation process. Excellent dispersions of the nanotubes in DNNSA-PANI were produced by horn sonication. First, SWNTs were dispersed in xylene and afterward sonicated into the DNNSA-PANI solution at a ratio by solids weight of 1:4. The coated tubes were then dispersed by sonication into a solution of the insulating host matrix at the desired concentrations. Thin films at the various SWNT concentrations were coated to approximately $1\ \mu\text{m}$ thickness onto glass slides with $1500\ \text{\AA}$ sputtered Ag contacts placed 1 cm apart. The conductivity was measured using a standard four-probe method.

Figure 1 shows the conductivity of DNNSA-PANI/SWNT at a 4:1 ratio embedded in a PS host (squares) and the conductivity of a DNNSA-PANI/SWNT (diamonds) as a function of SWNT concentration. The nanotube concentration was varied from 0% to 20% by weight. As shown in the Fig. 1, both networks, whether in conducting or insulating matrix, percolate at about 0.25% SWNT at the conductivity of their corresponding host, 10^{-4} and $10^{-8}\ \text{S/cm}$ for DNNSA-PANI and PS, respectively. The curves become essentially undistinguishable above 1%–2% SWNT content extrapolating to the conductivity of SWNT ropes at 100% loading.¹⁴⁻¹⁷

^{a)} Author to whom correspondence should be addressed; electronic mail: graciela.b.blanchet@usa.dupont.com

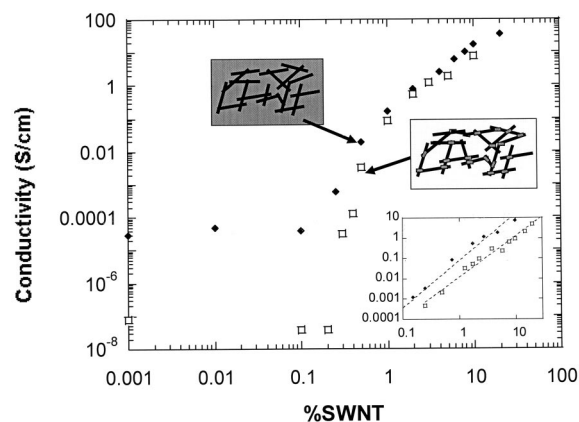


FIG. 1. Conductivity of self assembled conducting network as a function of the SWNT concentration. The diamonds and squares represent the conductivity of DNNSA-PANI coated SWNT in a DNNSA-PANI host and in a PS host, respectively. The SWNT content was varied from 0.1% to 20% by weight SWNT content. A schematic representation of each network is shown. The inset shows a log-log plot of the conductivity as a function of $c - c_c$ where c_c is the critical concentration ($c_c = 0.25\%$). The slope of the curves are 2.12 and 2.32 for the SWNT/DNNSA-PANI and DNNSA-PANI/SWNT in a PS host, respectively. A scaling exponent of approximately two is consistent with the expected behavior of a three-dimensional system as the system evolves from a neat polymeric host to a percolated network of nanotubes effectively connected with a low resistance joint, DNNSA-PANI.

In order to understand the network assembly properties, we characterized the structure of the samples by transmission electron microscopy (TEM). A Philips CM-20 ultrahigh-resolution TEM operated at 200 kV was equipped with a Link energy dispersive spectroscopy (EDS) system for elemental analysis using electron probe sizes that were less than 5 nm. DNNSA-PANI/SWNT and DNNSA-PANI/SWNT in PS samples with 3% SWNT contents were dispersed in xylene. Drops of these dispersions were placed on carbon-coated 200-mesh Cu TEM grid and dried under ambient conditions. Thin sections of the dried material projecting over the holes of the supporting carbon films were imaged as well as analyzed by small-probe EDS for elemental signatures.

Figure 2(a) is a high-resolution TEM image of bundles of SWNT in DNNSA-PANI. The dark particles visible in the image are carbon-encapsulated nanoparticles of iron catalyst

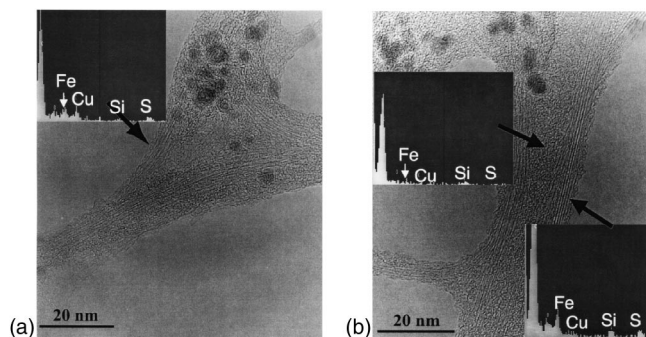


FIG. 2. High-resolution TEM images of bundles of DNNSA-PANI coated SWNT in (a) DNNSA-PANI and (b) PS hosts. The dark particles visible in the image are carbon-encapsulated nanoparticles of iron catalyst used in the HiPCO process. The attached EDS spectrums, shown as insets, reflect the compositional analysis of the material at the position of the arrow. The presence of small amounts of sulfur associated with the tubes is consistent with the presence of DNNSA-PANI. The spectra at the PS host 10 nm from the tubes show that no sulfur and thus no DNNSA-PANI are present.

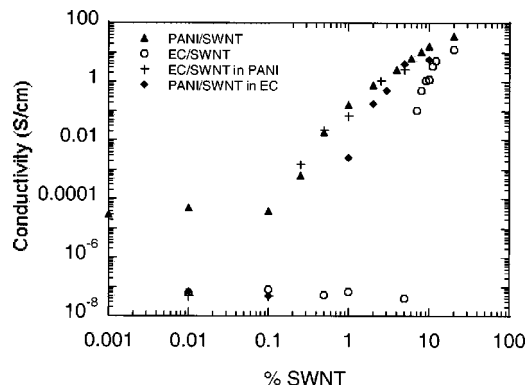


FIG. 3. Conductivity of self-assembled conducting network as a function of the SWNT concentration. The data shown as a filled triangle and circles correspond to the conductivity of DNNSA-PANI/SWNT and EC/SWNT networks, respectively, as a function of SWNT concentration. The SWNT content was varied from 0.1% to 20% SWNT content. The data shown as square and diamonds correspond to the conductivity of EC/SWNT in a DNNSA-PANI host and DNNSA-PANI /SWNT in an EC host vs SWNT content.

used in the HiPCO process.¹⁷ The images perhaps also suggesting that DNNSA-PANI might partially attack the bundles fracturing some of the tubes. The attached EDS spectrum shows the presence of small amounts of sulfur associated with the tubes, which is consistent with the sulfonyl groups present in DNNSA-PANI. Figure 2(b) is a high-resolution TEM image of the DNNSA-PANI/SWNT network in a PS host. The image, which is typical of these samples, illustrates areas with coated SWNT and as well as areas essentially composed of the PS hosts. The attached EDS spectra clearly indicate the presence of sulfur (S) in the vicinity of the SWNT bundles, but there is no evidence of S in the areas where the SWNT are not present. Since the S signal is ascribed to the DNNSA-PANI, these data suggest that the DNNSA-PANI is localized around the SWNT bundles and does not associate with the PS host.

Figure 3 illustrates the network self-assembling when conducting DNNSA-PANI and host compete for network links. Curves a (triangles) and b (circles) show the conductivity of SWNT/ethyl cellulose (EC) and DNNSA-PANI/SWNT networks, respectively. As expected from rods in an insulating matrix, SWNT linked with EC percolate at about 8% while SWNT linked with DNNSA-PANI matrix percolate at 0.25%.⁵ The large difference in percolation thresholds illustrate the importance of the resistance at the joints. When SWNT are connected via low resistance DNNSA-PANI links, it percolates into a conducting regime at a 30× lower threshold than when connected via insulating EC links.

Naturally, when a self-assembled DNNSA-PANI/SWNT network is dispersed in an EC host, the percolation threshold downshifts by almost an order of magnitude to ~1% [Figure 3(c) (squares)]. However, this value, representing a four-fold increase in percolation threshold relative to the PS counterpart, suggests that while PS does not displace DNNSA-PANI intertube joints, EC does. Then, as EC joints replace DNNSA-PANI at tube interconnects, there is an increase in network resistance and an upward shift in the percolation threshold. The competition between PANI and EC for the tube surface is further illustrated in Fig. 3(d) (diamonds) showing that when a self-assembled EC/SWNT is dispersed into a conducting DNNSA-PANI host, the percolation threshold shifts down to 0.25%. This result suggests that the EC links connecting the tubes have been fully replaced by

DNNSA-PANI, a low resistance SWNT “glue” that enables the self-assembly of highly conducting networks at a low percolation threshold.

Clear quantitative descriptions of the transport in poorly defined material systems, such as acid-doped PANI or mats and ropes of nanotubes in an insulating matrix, are difficult to develop.^{13–22} Even more problematic is the description of a composite of the three. Nevertheless, we do believe that there are some conclusions that can be drawn from a consideration of our data.

Although a large amount of work has gone into understanding the transport in heterogeneous systems, such as polymers, conducting polymers and nanotube mats,^{13–22} it has focused on understanding each separately rather than combined. The natural approach here is to consider that the conductivity of the self-assembled percolating network of DNNSA-PANI ($\sigma \sim 10^{-4}$ S/cm) and SWNT ropes ($\sigma \sim 10^2$ S/cm) embedded in an insulating host (PS $\sigma \sim 10^{-8}$ S/cm) is only controlled by the network and essentially independent of the PS host. Then, the scaling conductivity σ can be expressed as $\sigma = \sigma_0(c - c_c)^\gamma$.²² Where σ is the conductivity of the high conductivity phase (SWNT), $c - c_c$ is the difference in concentration of SWNT relative to the percolation concentration and γ is the critical exponent, a universal parameter reflecting the dimensionality of the network above percolation. Critical exponents of 2.12 and 2.32 are obtained from the slope of $\log \sigma$ as a function of $\log(c - c_c)$ (where $c_c = 0.25\%$) for SWNT/DNNSA-PANI and DNNSA-PANI/SWNT network in a PS hosts, respectively (inset of Fig. 1). These values are consistent with the formation of a three-dimensional network as the system evolves from a neat polymeric host to a percolating network of nanotubes effectively connected with a low resistance joint, DNNSA-PANI.

It is interesting to compare this behavior with that of SWNT in an EC host shown in Fig. 3. In this case, the scaling behavior is not seen as clearly. This is interesting data merely reflecting the effect of the internanotube resistance. In spite of the excellent dispersability and wetting of nanotubes in EC, the percolation threshold shifts from 0.25% when the nanotubes are connected with PANI to 7% when the internanotube connect is EC. This small layer of polymer between the tubes then acts as a large tunneling barrier, which is difficult to eliminate until rather high concentrations of nanotubes are reached. In addition, as the insulating host competes for the nanotube surface, partially or totally replacing the material at the joint, a shift in percolation threshold is observed. Replacing PANI with EC leads to higher intertube resistivity and an upward shift in percolation threshold. In contrast, when the EC interconnects sites are totally displaced by DNNSA-PANI a downward shift of the threshold is observed.

One can then propose that the Kaiser model describes transport above percolation;^{16,17} consistent with charge transport occurring mainly along a self-assembled network of DNNSA-PANI connected metallic tubes providing a path of

low contact resistance for intertube charge transfer.

To conclude, we have achieved the self-assembly of single-wall nanotubes ropes into three-dimensional conducting networks within an insulating matrix. This highly conducting filamentary structure made from organic materials provides opportunities for applications in micro- and nano-electronics. The unique combination of starting materials allowed for the self-assembly of SWNT ropes into a highly conducting network embedded in an insulating host without disrupting the conduction path. Our approach enables us to decouple the electrical properties of the links from those of the host. Conducting polymers provide low resistance self-assembled joints that effectively connect SWNTs. In a host with poor nanotube affinity, the conducting network is embedded into the host without disruption. The ability to control network formation independently of the host drastically changes the design of organic conducting networks. While, self-assembled networks of SWNT ropes are suitable conductors for TFT applications, self-assembled single tube networks may provide a similarly viable path to nanowire fabrications. Furthermore, the ability of self-assembling networks of single semiconducting tubes may play an important role in nanoscale electronic devices.

The authors thank Dr. Feng Gao for the synthesis of doped polyaniline.

¹H. Siringhaus *et al.*, *Science* **290**, 2123 (2000).

²J. A. Rogers *et al.*, *Proc. Natl. Acad. Sci. U.S.A.* **98**, 4835 (2001).

³C. J. Drury, C. M. J. Mutsaers, C. M. Hart, M. Hatters, and D. M. de Leeuw, *Appl. Phys. Lett.* **73**, 108 (1998).

⁴C. D. Dimitrakopoulos and P. R. L. Malenfant, *Adv. Mater. (Weinheim, Ger.)* **14**, 99 (2002).

⁵G. B. Blanchet, Y. L. Loo, J. A. Rogers, C. R. Fincher, and F. Gao, *Appl. Phys. Lett.* **82**, 463 (2003).

⁶G. Blanchet, C. R. Fincher, and F. Gao, *Appl. Phys. Lett.* **82**, 1290 (2003).

⁷J. C. Chiang, A. G. MacDiarmid, *Synth. Met.* **13**, 193 (1986).

⁸Y. Yao, P. Smith, and A. Heeger, *Synth. Met.* **48**, 91 (1992).

⁹M. Reghu, Y. Cao, D. Moses, and A. J. Heeger, *Phys. Rev. B* **47**, 1758 (1993).

¹⁰A. J. Epstein and A. G. MacDiarmid, *Synth. Met.* **69**, 179 (1995).

¹¹C. Y. Yang, M. Reghu, A. J. Heeger, and Y. Cao, *Synth. Met.* **79**, 27 (1996).

¹²G. B. Blanchet, C. R. Fincher, M. Lefenfeld, and J. A. Rogers, *Appl. Phys. Lett.* **84**, 296 (2004).

¹³P. J. Kinlen, U.S. Patent No. 5,863,465 (1999).

¹⁴H. Kataura, Y. Kumazawa, Y. Maniwa, I. Umezumi, S. Susuki, Y. Ohtsuka, and Y. Aciba, *Synth. Met.* **103**, 2555 (1999).

¹⁵P. Petit, C. Mathis, C. Journet, and P. Bernier, *Chem. Phys. Lett.* **305**, 370 (1999).

¹⁶A. B. Kaiser, G. Dusberg, and S. Roth, *Phys. Rev. B* **57**, 1418 (1998).

¹⁷J. E. Fisher, H. Dai, A. Thess, R. Lee, N. M. Hanjani, D. L. Dehaas, and R. E. Smalley, *Phys. Rev. B* **55**, R4921 (1997).

¹⁸R. S. Kohlman, A. Zibold, D. B. Tanner, G. G. Ihas, T. Ishigure, Y. G. Min, A. G. MacDiarmid, and A. J. Epstein, *Phys. Rev. Lett.* **78**, 3915 (1997).

¹⁹A. G. MacDiarmid and A. J. Epstein, *Synth. Met.* **65**, 103 (1994).

²⁰K. Lee and A. J. Heeger, *Synth. Met.* **84**, 715 (1997).

²¹J. P. Pouget, M. E. Jozefowicz, A. J. Epstein, X. Tang, and A. G. MacDiarmid, *Macromolecules* **24**, 779 (1991).

²²M. Sahimi, *J. Phys. A* **A17**, L165 (1984).